MECHANICAL VS EMPIRICAL MODELS FOR MODELS IN-PLANE RESPONSE OF INFILLED FRAMES: RELIABILITY COMPARISON AND VALIDATION OF A NEW DATA-DRIVEN MODEL

Fabio Di Trapani[1*]**, Giovanni Tomaselli**[1]**, and Gabriele Bertagnoli**[1]

[1] Politecnico di Torino
Dipartimento di Ingegneria Strutturale Edile e Geotecnica
Corso Duca degli Abruzzi 24
{ fabio.ditrapani, giovanni.tomaselli, gabriele.bertagnoli}@polito.it

Abstract

The paper proposes a new quadri-linear empirical force-displacement relationship to model the inelastic response of infill equivalent struts. The definition of the model is based on a data-driven approach rather than a mechanical one, therefore parameters defining the force-displacement curve are analytically evaluable by means of empirical correlations. The latter link the force-displacement parameters regulating the axial response to the geometrical and mechanical features of an infilled frame. The analytical correlations are obtained from an experimental data-set enlarged with data from refined finite element simulations. Blind validation tests of the proposed modelling procedure are carried out against experimental results different from those used to build the data-set. A reliability comparison between mechanics-based models and empirical models is finally presented and discussed.

Keywords: OpenSees, empirical, FEM, Masonry, Infilled Frames, Reinforced concrete, Data-driven

1 INTRODUCTION

Infill-frame interaction has been largely investigated during last 60 years by researchers from all over the world. Despite this, the interest devoted to this topic is still noticeable. This can be easily observed, for example, by the experimental activity, which continues nowadays. In fact, besides the availability of a number of in-plane experimental tests (e.g. [1- 7]), several new ones have been performed out only recently (e.g. [8-14]). In the same period, thanks to the improvements in the efficiency of computational capacity of computers and software, in-depth numerical studies were also addressed to assess the global influence of infills in seismic response of building frames [15-23] or local interaction issues [24-28].

Comparing an overview of past and recent literature on in-plane equivalent strut modelling of infilled frames, it results that predictions from different models lead to results which are many times conflicting [16,29-32], raising doubts on the reliability of the different models. One of the possible reasons is the fact that most of the force-displacement relationships used to model the response of the equivalent struts, are based on mechanical approaches, which are typically a consequence of supposing limit equilibrium conditions. Unfortunately, this way of approaching this problem may fail in accuracy if the actual collapse mechanism is different from the one assumed. Another reason is that most of past design equations were calibrated on the experimental knowledge available in a previous period or for a specific typology of infills. Based on these premises, this paper first presents a new equivalent strut macro-model, which is defined using an empirical data-driven approach. A typical quadri-linear axial-force/axial-displacement relationship is proposed for the axial response of the struts. The force-displacement model is simply ruled by four parameters modulating the cracking strength, the post-cracking stiffness, the softening branch, and the residual strength peak strength. Analytical expressions for these parameters are derived in the paper making use of a hybrid experimental/numerical data-set, built after an iterative calibration process of the equivalent strut models on real experimental tests and additional finite element simulations. The four analytical correlation laws directly link geometrical and mechanical properties of an infilled frame to four parameters (called force-displacement parameter) regulating the force-displacement relationship. Blind validation tests of the model are carried out against eight different experimental test data, not belonging to those used to build the data-set used to derive the correlation laws. The proposed model predictive capacity is also compared to that of other six literature models making consideration about the different reliability of mechanics based and empirical based formulations.

2 PROPOSED EQUIVALENT STRUT MODEL

2.1 Computational model and formulation

The computational scheme of the proposed model refers to the classical configuration of a pair of compression-only concentric equivalent struts (**Fig. 1a**). Beam and column elements are modelled using distributed plasticity fiber-section elements. The equivalent strut elements are modelled as trusses with inelastic force-displacement behaviour, characterized by the axial force – axial displacement behaviour illustrated in **Fig. 1b**. In the current study, the *OpenSees* software platform [34] is used to perform modeling and simulations. The *Pinching 4* material is used to model the axial response of the struts. However, this modelling strategy can be easily reproduced with any structural software handling nonlinear analysis of frame structures, using multilinear plastic links as shown by [11].
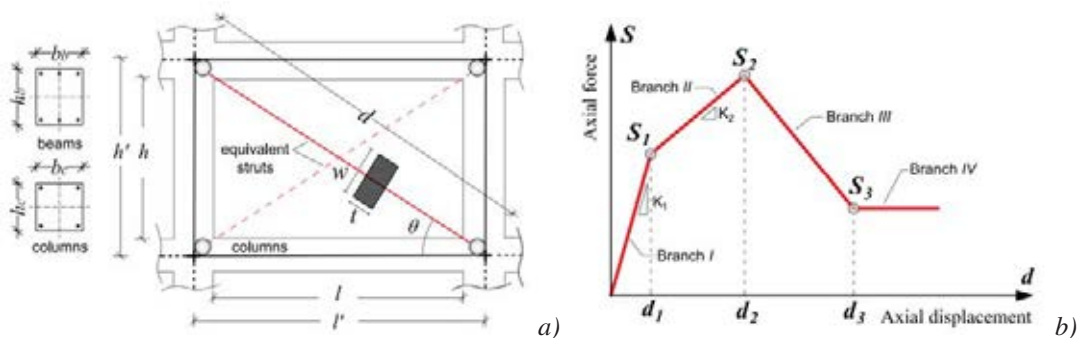

Figure 1. Equivalent strut modelling of the fame-infill system: a) Geometric configuration; b) Proposed axial force – axial displacement model for the struts.

The shape of the inelastic relationship for the strut is the same as the one proposed by other authors (e.g. [35,36]). The latter provides an initial uncracked branch up to the point S_1-d_1, characterized by the stiffness K_1, a second cracked stiffness branch up to the peak point S_2-d_2, having stiffness K_2, a third softening branch and a fourth residual strength branch starting in correspondence of the point S_2-d_3. The latter branch can be considered having unlimited or specified deformation threshold. The force-displacement is defined as follows.

Branches 1 and 2, are evaluated similarly to what provided by [11] and [37], therefore, the initial stiffness (branch I) is defined as:

$$K_1 = \frac{\tilde{E}_m tw}{d} \tag{1}$$

where t, w and d are the thickness, the width and the length of the diagonal strut and $\tilde{E}_m$ is the conventional elastic modulus, defined as [33]:

$$\tilde{E}_m = \sqrt{E_{m1} \cdot E_{m2}} \tag{2}$$

in which E_{m1} and E_{m2} are the Young moduli of masonry along the horizontal and vertical direction respectively. As regards the identification of the equivalent strut cross-section width (w), this is performed by following the procedure proposed by [33]. The stiffness of branch II is related to the stiffness K_1 by the parameter β (≤ 1) as:

$$K_2 = \beta K_1 \tag{3}$$

The peak strength S_2 can be considering S_2 as the product of the diagonal peak resistance of the strut (f_{md0}) and the area of its cross section, namely:

$$S_2 = f_{md0} tw \tag{4}$$

where f_{md0} can be analytically evaluated as provided by [33]. Once evaluated S_2, the peak strength S_1 is defined through the parameter α (≤ 1) as:

$$S_1 = \alpha S_2 \tag{5}$$

The cracking and peak displacements are then defined as:

$$d_1 = \frac{S_1}{K_1}; \qquad d_2 = d_1 + \frac{S_2 - S_1}{K_2} \tag{6}$$

The softening branch is obtained as a linearization of the exponential softening branch proposed by [37]. This is done connecting the point S_2-δ_2 and the auxiliary point S_3^*-d_3^* (**Fig. 2a**), where for S_3^* it is conventionally set $S_3^* = 0.7 S_2$, and d_3^* is obtained through the expression [11] (**Fig. 2b**):

$$d_3^* = \frac{1}{\zeta} ln \left[\frac{S_2}{S_3^*} exp(\zeta d_2) \right] \tag{7}$$

in which ζ is one of the empirical parameters to be calibrated.

Finally, the residual strength (S_3) is related to the peak strength by the parameter η (≤ 1) as:

$$S_3 = \eta S_2 \tag{8}$$

The displacement at which the constant branch starts is obtained as interception of the lines identifying the branches II and IV, which results from the following equation:

$$d_3 = d_2 + (\eta - 1) \left(\frac{d_3^* - d_2}{S_3^* - S_2} \right) S_2 \tag{9}$$
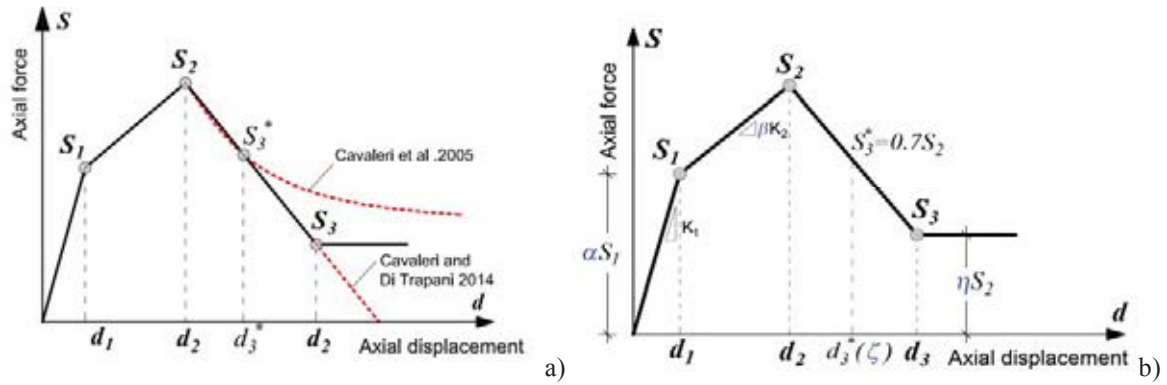
Figure 2. Force-displacement relationship for the equivalent strut: a) Comparison with **Cavaleri et al.** [38] and **Cavaleri and Di Trapani** [11] relationships; b) Calibrations parameters.

According to previous equations the force-displacement response is defined once the four parameters α, β, ζ, and η (called "force-displacement parameters") are defined. These parameters have a strict dependence on masonry mechanical properties, but, more in general, their values depend on geometrical and mechanical features of the whole infilled frame. Their determination is possible by the empirical analytical correlations derived in the following sections.

3 CALIBRATION OF FORCE-DISPLACEMENT PARAMETERS FROM EXPERIMENTAL TESTS

The reference specimens are selected from the experimental tests by [2,5,6,7,11]. Geometric and typological details of specimens are reported in **Table 1**, while the other mechanical properties are shown in **Table 2**, together with the equivalent strut cross-section widths and the other parameters evaluated for the identification of the struts.

The simulation of the tests was carried out in OpenSees by conducting simple pushover analyses of the equivalent strut model of each specimen. The calibration process was performed by comparing the obtained monotonic force-displacement curves with the backbone curves of the cyclic experimental responses. Results are shown in **Figures 3-7**, where numerical pushover curves at the end of the calibration process, and the experimental results (positive and negative backbone curves) are overlapped.

The experimental values of masonry shear strength (f_{vm}) and compressive strength along orthogonal directions (f_{m1} and f_{m2}) are reported in **Table 3** together with the conventional compressive strength ($\tilde{f}_m$) defined as [33]:

$$\tilde{f}_m = \sqrt{f_{m1} \cdot f_{m2}} \qquad (10)$$

and the diagonal compressive strength (f_{md0}) of the equivalent struts.

References	Spec. #	Masonry units type	t (mm)	h (mm)	h' (mm)	l (mm)	l' (mm)	l/h (-)	d (mm)	b_c (mm)	h_c (mm)	b_b (mm)	h_b (mm)
Cavaleri & Di Trapani [11]	S1A	Calcarenite	200	1600	1800	1600	1800	1.00	2545.6	200	200	200	400
Cavaleri & Di Trapani [11]	S1B	Clay / hollow	150	1600	1800	1600	1800	1.00	2545.6	200	200	200	400
Mehrabi et al. [2]	4	Brick / hollow	92	1422	1536	2032	2210	1.43	2691.5	178	178	152.4	228.6
Mehrabi et al. [2]	5	Brick / solid	92	1422	1536	2032	2210	1.43	2691.5	178	178	152.4	228.6
Mehrabi et al. [2]	11	Brick / solid	92	1422	1536	2948	3126	2.07	3483.1	178	178	152.4	228.6
Mehrabi et al. [2]	6	Brick / hollow	92	1422	1536	2032	2235	1.43	2712.3	203.2	203.2	152.4	228.6
Kakaletsis& Karayannis [7]	S	Brick	60	800	900	1200	1350	1.50	1622.5	150	150	100	200
Papia et al. [5]	S2A	Calcarenite	200	1600	1800	1600	1800	1.00	2545.6	200	200	200	400
Papia et al. [5]	S2B	Clay / hollow	150	1600	1800	1600	1800	1.00	2545.6	200	200	200	400
Colangelo [6]	C1	Clay / hollow	120	1300	1425	1700	1900	1.31	2375.0	200	200	200	250
Colangelo [6]	L2	Clay / hollow	120	1300	1425	2300	2500	1.77	2877.6	200	200	200	250
Colangelo [6]	N1	Clay / hollow	160	1300	1425	2300	2500	1.77	2877.6	200	200	200	250

Table 1. Geometric and typological details of reference specimens.

References	Spec. #	F_v (kN)	E_{m2} (MPa)	E_{m1} (MPa)	$\tilde{E}_m$ (MPa)	E_c (MPa)	ν (-)	c (-)	β (-)	ε_v (%)	κ (-)	γ (-)	λ^* (-)	w (mm)
Cavaleri & Di Trapani [11]	S1A	400	3933	7408	5397	25000	0.150	0.260	0.150	0.20	1.048	1.50	2.186	631.4
Cavaleri & Di Trapani [11]	S1B	400	6040	5070	5697	25000	0.100	0.254	0.148	0.20	1.046	1.50	1.730	636.8
Mehrabi et al. [2]	4	294	4600	4600	4600	17000	0.150	0.260	0.150	0.27	1.059	3.08	0.978	587.1
Mehrabi et al. [2]	5	294	8949	8949	8949	18064	0.150	0.260	0.150	0.26	1.060	3.08	1.791	536.6
Mehrabi et al. [2]	11	294	9604	9604	9604	18133	0.150	0.260	0.150	0.26	1.059	10.24	1.664	726.7
Mehrabi et al. [2]	6	294	4198	4198	4198	19856	0.150	0.260	0.150	0.18	1.038	3.08	0.654	590.1
Kakaletsis & Karayannis [7]	S	100	670.3	660.7	665.5	29961	0.150	0.260	0.150	0.07	1.015	3.53	0.046	470.5
Papia et al. [5]	S2A	400	7106	9528	8228	23000	0.090	0.253	0.148	0.22	1.058	1.50	3.622	578.2
Papia et al. [5]	S2B	400	6040	5070	5697	23000	0.100	0.254	0.148	0.22	1.051	1.50	1.881	633.1
Colangelo [6]	C1	400	4230	1688	2672	34200	0.100	0.254	0.148	0.15	1.030	2.46	0.277	598.8
Colangelo [6]	L2	400	4230	1688	2672	35417	0.100	0.254	0.148	0.14	1.029	5.90	0.218	610.8
Colangelo [6]	N1	400	1212	2623	1782	34429	0.100	0.254	0.148	0.15	1.030	5.90	0.199	621.6

Table 2. Equivalent strut widths and associate ed mechanical data.
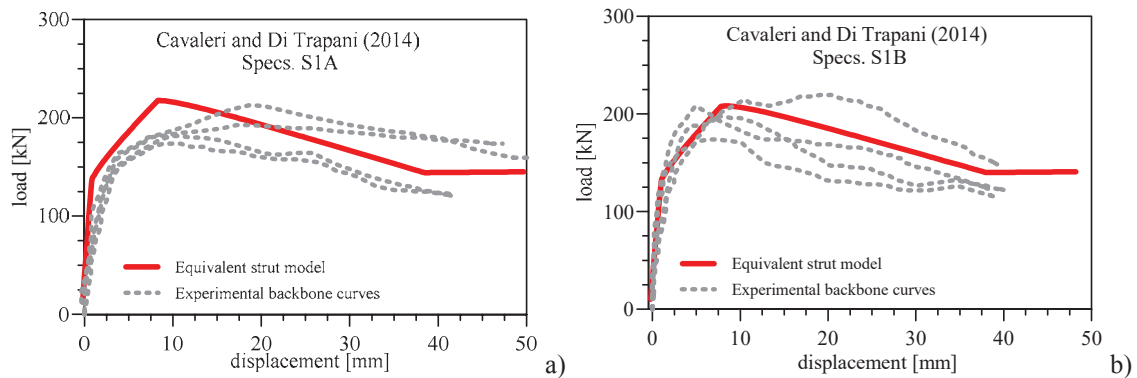

Figure 3. Experimental backbone curves by **Cavaleri and Di Trapani** [11] and pushover curves of the equivalent strut infilled frame model after the calibration: a) Specimens S1A; b) Specimens S1B.
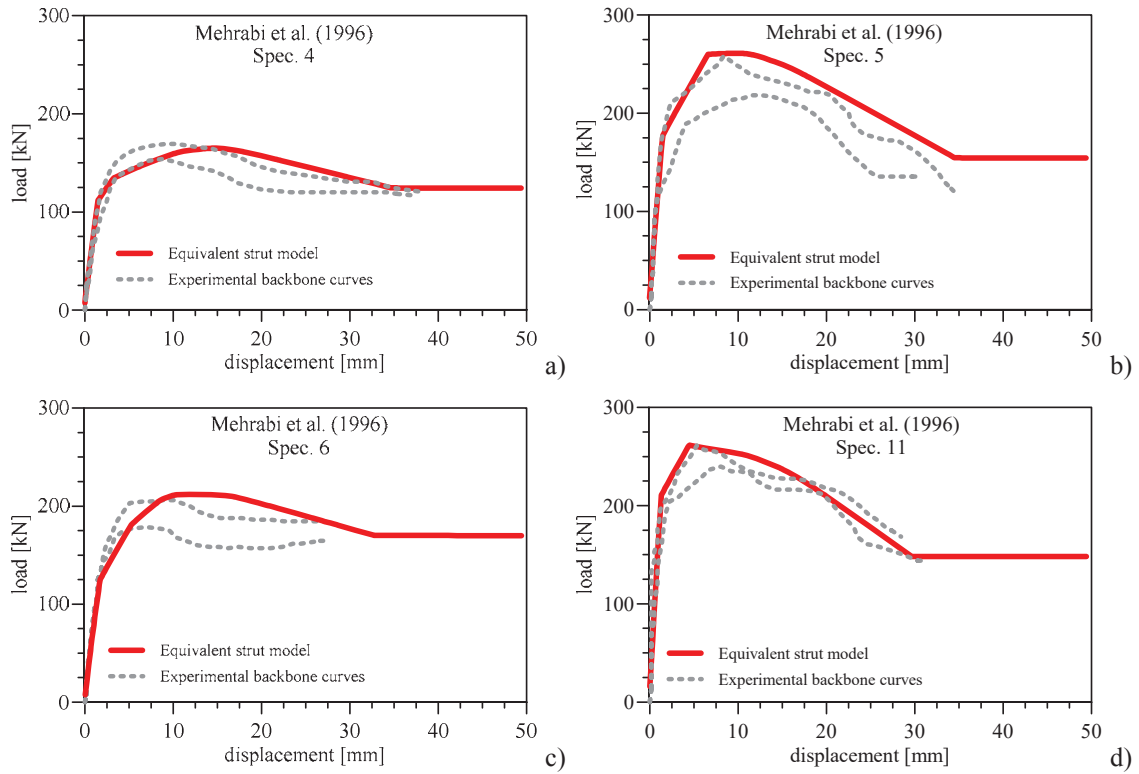
Figure 4. Experimental backbone curves by **Mehrabi et al.** [2] and pushover curves of the equivalent strut infilled frame model after the calibration: a) Specimen 4; b) Specimen 5; c) Specimen 6; d) Specimen 11.
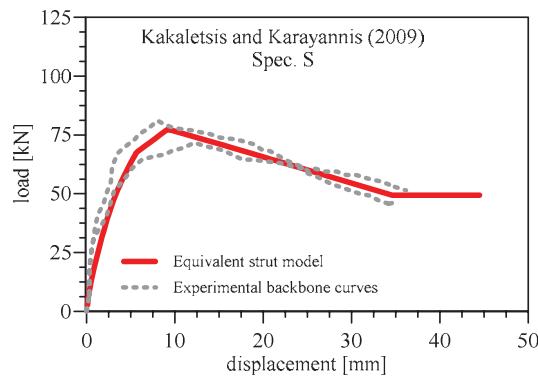

Figure 5. Experimental backbone curves by **Kakaletsis et al.** [7] and pushover curves of the equivalent strut infilled frame model after the calibration.
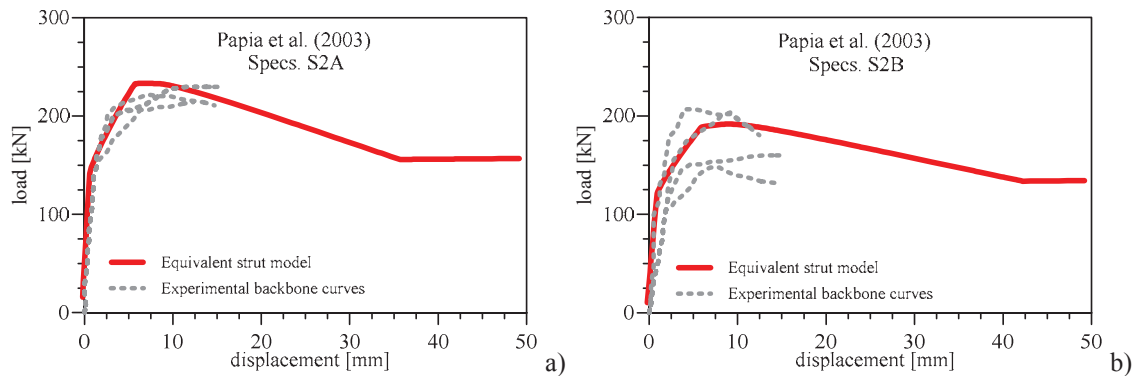

Figure 6. Experimental backbone curves of specimens by **Papia et al.** [5] and pushover curves of the equivalent strut infilled frame model after the calibration: a) Specimens S2A; b) Specimens S2B.
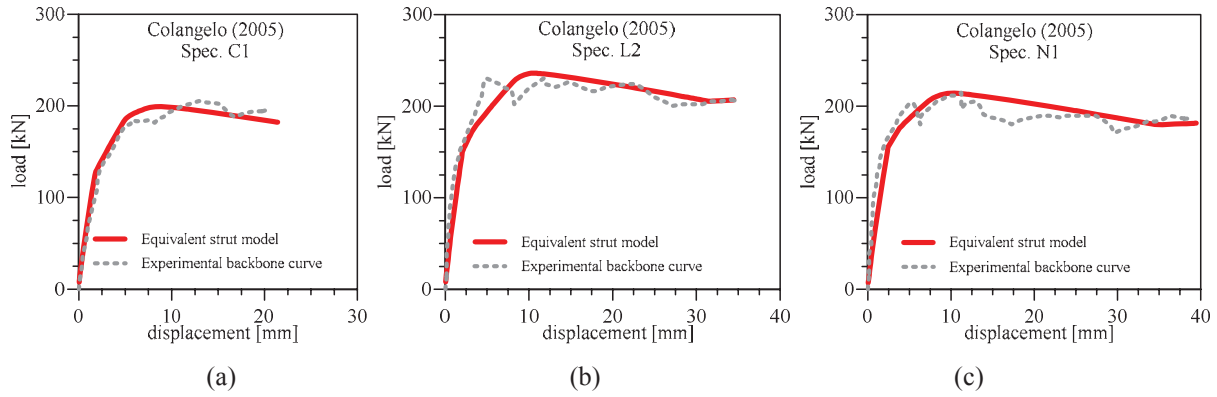
Figure 7. Experimental backbone curves by **Colangelo** [6] and pushover curves of the equivalent strut infilled frame model after the calibration: a) Specimen C1; b) Specimen L2; c) Specimen N1.

The optimal force-displacement parameters (α, β, ζ and η) obtained after the calibration are finally reported in **Table 4** together with the resulting force-displacement values for the struts.

References	Spec. #	f_{vm} (MPa)	f_{m2} (MPa)	f_{m1} (MPa)	$\widetilde{f}_m$ (MPa)	f_{md0} (MPa)
Cavaleri & Di Trapani [11]	S1A	0.73	2.67	3.08	2.86	2.0
Cavaleri & Di Trapani [11]	S1B	1.07	8.70	4.18	6.00	2.5
Mehrabi et al. [2]	4	0.93	5.09	2.75	3.74	2.4
Mehrabi et al. [2]	5	1.15	13.84	13.84	13.84	5.3
Mehrabi et al. [2]	11	1.03	11.44	11.44	11.44	3.8
Mehrabi et al. [2]	6	0.7	4.86	2.62	3.57	2.6
Kakaletsis & Karayannis [7]	S	0.08	5.11	2.63	3.66	2.3
Papia et al. [5]	S2A	0.89	4.57	3.92	4.23	2.5
Papia et al. [5]	S2B	1.07	8.70	4.18	6.00	2.3
Colangelo [6]	C1	0.87	5.10	3.39	4.15	2.05
Colangelo [6]	L2	0.87	5.10	3.39	4.15	1.8
Colangelo [6]	N1	0.58	2.74	3.90	3.24	1.4

Table 3. Experimental mechanical data of masonry and resulting conventional and diagonal strengths.

References	Spec. #	α -	β -	ζ -	η -	S_1 (kN)	d_1 (mm)	S_2 (kN)	d_2 (mm)	S_3 (kN)	d_3 (mm)
Cavaleri & Di Trapani [11]	S1A	0.7	0.06	0.030	0.50	176.8	0.66	252.6	5.38	176.8	25.2
Cavaleri & Di Trapani [11]	S1B	0.7	0.08	0.030	0.50	167.2	0.78	238.8	4.97	167.2	24.8
Mehrabi et al. [2]	4	0.9	0.10	0.033	0.30	116.7	1.26	129.6	2.67	90.7	27.9
Mehrabi et al. [2]	5	0.75	0.10	0.037	0.30	196.2	1.20	261.6	5.18	183.2	27.7
Mehrabi et al. [2]	11	0.85	0.075	0.040	0.25	215.9	1.17	254.0	3.93	177.8	26.2
Mehrabi et al. [2]	6	0.85	0.09	0.035	0.35	119.9	1.43	141.1	4.23	98.8	26.3
Kakaletsis & Karayannis [7]	S	0.8	0.70	0.035	0.40	519.4	4.52	64.9	6.14	45.4	26.5
Papia et al. [5]	S2A	0.65	0.09	0.030	0.50	187.9	0.50	289.1	3.51	202.4	23.3
Papia et al. [5]	S2B	0.7	0.10	0.025	0.50	152.9	0.72	218.4	3.80	152.9	27.6
Colangelo [6]	C1	0.8	0.15	0.030	0.50	117.8	1.46	147.3	3.89	103.1	23.7
Colangelo [6]	L2	0.95	0.10	0.030	0.40	125.3	1.84	131.9	2.81	92.3	26.6
Colangelo [6]	N1	0.95	0.10	0.025	0.45	132.3	2.15	139.2	3.28	97.5	29.4

Table 4. Parameters α, β, ζ and η after the calibration and resulting force and displacement values for the struts.

4   FORCE-DISPLACEMENT PARAMETERS CALIBRATION FROM FE MODELS

In order to enlarge the data-set, additional numerical tests were considered by taking those provided by [33]. The latter are obtained through a refined FE model experimentally validated and implemented in the ATENA 2D software platform. A view of the reference FE model is illustrated in **Fig. 8a**. The comparison between the FE model prediction and the reference experimental tests used for the validation (Specs. S1B by[11]) is also shown in **Fig. 8b**.
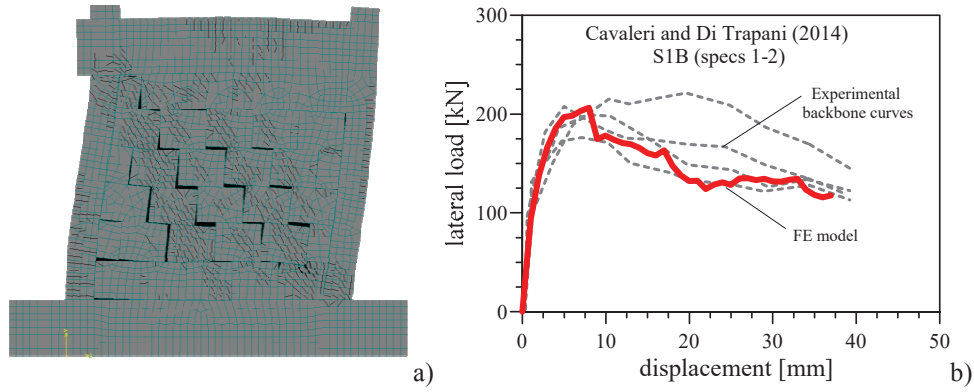
Figure 8. Reference FE model: a) View of the model during a typical pushover test; b) Comparison between FE model prediction and experimental backbone curves of specimens S1B (**Cavaleri and Di Trapani** [11]).

Numerical tests specimens extrapolated by the reference FE model were obtained by varying compressive and tensile strength of masonry (f_m and f_{vm}), infill thickness (t) and masonry elastic Young's modulus (E_m). The interface and concrete parameters were instead maintained fixed, as well as the geometry of the frame (spec. S1B by [11]). The geometrical and mechanical parameters which were varied to generate the numerical models are reported in **Table 5**, highlighting those each time varied. The infilled frame equivalent strut models associated with the generated FE models were then built and calibrated to derive force-displacement parameters as shown in the previous section. Force-displacement curves at the end of the calibration are depicted **Fig. 9** together with the respective force-displacement curves of the FE model simulations. Parameters evaluated at the end of the calibration and related force-displacement parameters obtained are finally reported in **Table 6** together with the resulting force-displacement values for the struts.
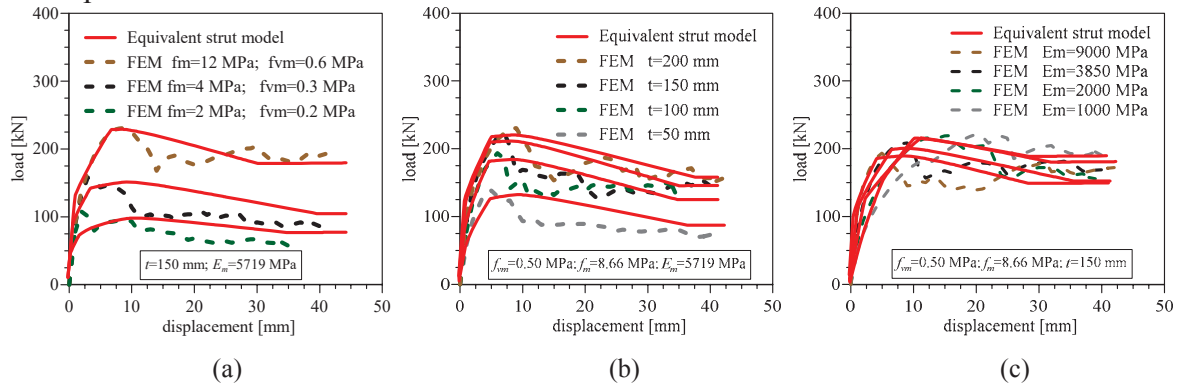

Figure 9. Force-displacement curves from FE models and equivalent strut models after the calibration: a) variation of masonry strength; b) variation of infill thickness; c) variation of elastic modulus.

Spec. #	f_{vm} (MPa)	$f_m = \tilde{f}_m$ (MPa)	t (mm)	$E_m = \tilde{E}_m$ (N/mm²)
FEM-1S	0.60	12.00	150	5719
FEM-2S	0.40	4.00	150	5719
FEM-3S	0.20	2.00	150	5719
FEM-1T	0.50	8.66	50	5719
FEM-1T	0.50	8.66	100	5719
FEM-1T	0.50	8.66	150	5719
FEM-1T	0.50	8.66	200	5719
FEM-1E	0.50	8.66	150	1200
FEM-2E	0.50	8.66	150	2000
FEM-3E	0.50	8.66	150	3850
FEM-4E	0.50	8.66	150	9000

Table 5. Geometric and mechanical data of numerical models generated from the S1B specimen model.

Spec.	λ^*	w	f_{md0}	α	β	ζ	η	S_1	d_1	S_2	d_2	S_3	d_3
	-	(mm)	(MPa)	-	-	-	-	(kN)	(mm)	(kN)	(mm)	(kN)	(mm)
FEM-1S	1.737	636.4	1.70	0.7	0.12	0.03	0.40	113.6	0.7	162.3	2.42	113.6	2.42
FEM-2S	1.737	636.4	2.90	0.6	0.15	0.027	0.60	166.1	0.6	276.8	4.22	193.8	4.22
FEM-3S	1.737	636.4	0.80	0.8	0.07	0.038	0.30	61.1	0.8	76.4	1.30	53.5	1.30
FEM-1T	0.579	744.3	3.50	0.5	0.3	0.040	0.30	65.1	0.5	130.3	3.38	91.2	3.38
FEM-1T	1.158	673.8	3.20	0.5	0.25	0.033	0.45	107.8	0.5	215.6	3.56	150.9	3.56
FEM-1T	1.737	636.4	2.70	0.6	0.16	0.030	0.50	154.7	0.6	257.8	3.73	180.4	3.73
FEM-1T	2.316	611.7	2.20	0.6	0.15	0.025	0.55	161.5	0.6	269.2	3.20	188.4	3.20
FEM-1E	0.608	739.2	2.20	0.6	0.18	0.022	0.75	146.4	0.6	243.9	7.90	170.7	7.90
FEM-2E	1.169	672.8	2.30	0.6	0.16	0.025	0.60	139.3	0.6	232.1	4.71	162.5	4.71
FEM-3E	0.304	817.7	2.00	0.7	0.4	0.02	0.80	171.7	0.7	245.3	7.38	171.7	7.38
FEM-4E	2.734	598.2	2.50	0.6	0.12	0.025	0.60	134.6	0.6	224.3	2.78	157.0	2.78

Table 6. Identification parameters of equivalent strut, parameters α, β, ζ and η after the calibration and resulting force and displacement values for the struts.

5 DEFINITION OF THE EMPIRICAL CORRELATION LAWS

The experimental and numerical data-sets containing the calibrated parameters α, β, ζ and η together with the associated geometrical and mechanical features of the respective infilled frames were merged in to a unique hybrid data-set. Results were then analysed in order to understand the dependence of α, β, ζ and η on the parameters involved in the identification process of each model. In detail parameters λ^*, $\tilde{E}_m$, (l/h), t, $\tilde{f}_m$, f_{md0}, f_{vm} where individuated as the most meaningful to the inelastic response of an infill frame, as these take into account the aspect ratio, the stiffness ratio and the strengths of the masonry and of the strut. The relationships with α, β, ζ and η have been found by defining four correlation parameters (A, B, Z and Y) to get the maximum determination coefficients (R^2) of the analytical interpolating functions relating α, β, ζ and η as $f(A)$, $f(B)$, $f(Z)$ and $f(Y)$. Results provided the following expressions for the correlation parameters:

$$A = \lambda^{*0.1}\left(\frac{l}{h}\right)^{-3}\left(\frac{f_{md0}}{f_{vm}^{0.4}}\right) \tag{11}$$

$$B = \lambda^{*0.7}\left(\frac{l}{h}\right)^{1.8}\left(\frac{f_{md0}^{-1.7}}{f_{vm}^{-0.7}}\right)\frac{1}{t^{0.5}} \tag{12}$$

$$Z = \left(\frac{\tilde{E}_m}{\tilde{f}_m}\right)^{0.7}\left(\frac{l}{h}\right)^{0.7}\left(\frac{f_{md0}^{0.7}}{f_{vm}^{0.35}}\right)\frac{1}{t} \tag{13}$$

$$Y = \left(\frac{\tilde{E}_m^{0.7}}{t}\right)\left(\frac{l}{h}\right)^{1.2}\left(\frac{\tilde{f}_m^{-0.5}}{f_{vm}^{0.1}}\right) \tag{14}$$

The relationships between parameters α, β, ζ and η and correlation parameters A, B, Z and Y are illustrated in **Fig. 10**, together with the obtained optimal analytical correlation laws.
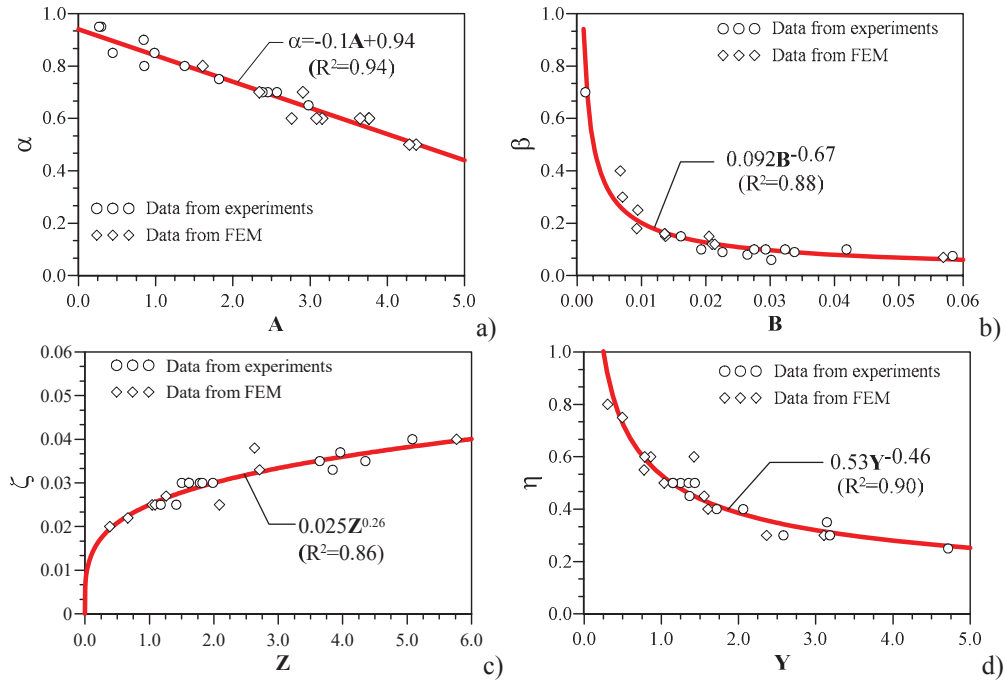
Figure 10. Relationships between parameters α, β, ζ and η and correlation parameters A, B, Z and Y and proposed analytical correlation laws.

Based on the obtained equations, the procedure for the complete identification of the equivalent strut follows the below reported steps:

1. Evaluation of the equivalent strut width w [33];
2. Evaluation of the peak strength of the strut S_2 (**Eq. 4**);
3. Evaluation of correlation parameters A, B, Z, Y (**Eqs. 12-15**);
4. Evaluation of force-displacement parameters α, β, ζ, η (**Fig.10**);
5. Determination of the force-displacement relationship for the strut (**Eqs. 1, 3** and **5-9**);

6   BLIND VALIDATION TESTS AND RELIABILITY COMPARISONS

The proposed empirical correlations have been validated with the experimental test results of eight specimens, not belonging to the set of specimens used to derive the correlations. The considered specimens were those by [14] (Spec. TA-2), [10] (Spec. URM-U), [6](Spec. V21), [12] (Spec. FT-2), [13] (Specs. GLD and SLD), [9] (Spec Unr), [11] (Spec S1C). With regards to the experimental campaign by [6], of which some specimens have been used to build the data-set, it should be specified that experimental results used for the validation are those of Specimen V21, which has not been previously considered and presents substantially different mechanical properties of the masonry infill with respect to those included in the data-set. The same considerations may be taken for the specimen S1C of the experimental campaign by [11]. The other six specimens belong to other experimental campaigns not considered at all in the calibration phase. It should be also specified that specimens GLD and SLD by Verderame et al. [13] have the same geometric and mechanical characteristics for what concerns the frame and the infill. The differences are instead in the arrangement of the longitudinal and transverse reinforcement that is made considering gravity loads only (GLD) or seismic loads (SLD). Geometric details of the specimens are listed in **Table 7**. Equivalent strut models have been defined according to the procedural steps described in the previous section. **Tables 7-9** collect all the fundamental geometric and mechanical data of the models and the associated parameters used for the definition of struts. The correlation and force-displacement param-

eters evaluated by means of **Eqs.** (**12-15**) and equation if **Fig. 10** are shown in **Tables 10-11**, together with the obtained values for the axial-force / axial-displacement relationship of the struts. The comparison between experimental force-displacement curves and numerical predictions are depicted in **Fig. 11**. It can be observed that for all the considered cases, numerical predictions resulted in a very good matching with experimental data, providing sufficient reliability despite the large heterogeneity of the blind test specimens and in consideration of the uncertainty degree affecting masonry mechanics in general and infilled frames in particular.

In order to compare the reliability of the proposed model predictive capacity with respect to that of other existing ones, the simulation of the blind tests has been conducted also implementing other six equivalent strut models available in the literature and applying them on the blind tests. The equivalent strut models are the models by Di Trapani et al.[33], Panagiotakos and Fardis [35], Dolsek and Fajfar [38], Bertoldi et al. [36], De Risi et al. [32], Sassun et al. [39]. The comparisons between the experimental test responses and those by the seven equivalent strut models are illustrated in **Fig. 11**.

References	Spec. #	Masonry units type	t (mm)	h (mm)	h' (mm)	l (mm)	l' (mm)	l/h (-)	d (mm)	b_c (mm)	h_c (mm)	b_b (mm)	h_b (mm)
Morandi et al. [14]	TA2	Clay Holl.	350	2950	3125	4220	4570	1.43	5536	350	350	350	350
Da Porto et al. [10]	URM-U	Clay Holl.	300	2650	2775	4150	4450	1.56	5244	300	300	300	250
Colangelo [6]	V21	Clay	160	1300	1425	2300	2500	1.76	2878	200	200	200	250
Bergami & Nuti [12]	-	Clay Holl.	120	1300	1425	2300	2500	1.76	2878	200	200	200	250
Verderame et al. [13]	GLD-SLD	Clay Holl.	80	1350	1475	2100	2300	1.55	2732	200	200	200	250
Sigmund & Penava [9]	Unr	Clay	120	1300	1400	1800	2000	1.38	2441	200	200	120	200
Cavaleri & Di Trapani [11]	S1C	Concrete	150	1600	1800	1600	1900	1.00	2617	300	300	300	400

Table 7. Geometric and typological details of the specimens used for the validation.

References	E_{m2} (MPa)	E_{m1} (MPa)	$\tilde{E}_{m1}$ (MPa)	G (MPa)	E_c (MPa)	f_{m2} (MPa)	f_{m1} (MPa)	$\tilde{f}_{m1}$ (MPa)	f_{vm} (MPa)	f_{md0} (MPa)
Morandi et al. [14]	5299	494	1618	2119.6*	30000	4.64	1.08	2.24	0.36	0.94
Da Porto et al. [10]	4312	1767	2760	1713	30000	6.00	1.19	2.67	0.2	1.15
Colangelo [6]	3188	3188	3188	1574	33900	2.24	2.56	2.39	0.35	1.58
Bergami & Nuti [12]	7228	4031	5398	4031	31475	6.19	2.91	4.24	1.26	2.41
Verderame et al. [13]	3940	3940	3940	1724.8*	27870	4.88	3.19	3.94	0.36	2.27
Sigmund & Penava [9]	3900	638**	1577	1560*	36283	2.7	0.44***	1.092	0.7	1.11
Cavaleri & Di Trapani [11]	4565	1944	2979	2042	25000	1.74	0.3	0.722	0.29	0.75

(*estimated as $0.4E_{m2}$; **estimated as $R_{b1}/R_{b2}E_{m2}$; ***estimated as $R_{b1}/R_{b2}f_{m2}$; R_{bi}=block resistance in direction 1-2)

Table 8. Experimental mechanical data of the specimens and evaluated mechanical properties.

References	F_v (kN)	ν -	c -	β -	κ -	γ -	λ^* -	w (mm)
Morandi et al. [14]	800	0.1	0.254	0.148	1.023	3.094	0.401	1203.34
Da Porto et al. [10]	800	0.17	0.263	0.151	1.032	4.007	0.740	1045.62
Colangelo [6]	400	0.10	0.254	0.148	1.030	5.899	0.362	571.98
Bergami & Nuti [12]	318	0.10	0.254	0.148	1.026	5.899	0.495	533.46
Verderame et al. [13]	200	0.10	0.254	0.148	1.018	3.928	0.302	571.26
Sigmund & Penava [9]	730	0.10	0.254	0.148	1.051	2.838	0.198	654.44
Cavaleri & Di Trapani [11]	400	0.10	0.254	0.148	1.018	1.500	0.392	783.39

Table 9. Equivalent strut widths and associated mechanical identification parameters.

References	A	B	Z	Y	α	β	ζ	η
	-	-	-	-	-	-	-	-
Morandi et al. [14]	0.440	0.029	0.503	0.573	0.899	0.097	0.021	0.685
Da Porto et al. [10]	0.553	0.027	1.139	1.052	0.888	0.103	0.026	0.518
Colangelo [6]	0.392	0.024	2.856	2.524	0.904	0.112	0.033	0.346
Bergami & Nuti [12]	0.371	0.041	3.166	3.214	0.906	0.078	0.034	0.310
Verderame et al. [13]	0.805	0.013	5.442	3.896	0.863	0.167	0.039	0.284
Sigmund & Penava [9]	0.411	0.034	2.080	2.115	0.902	0.087	0.030	0.376
Cavaleri & Di Trapani [11]	1.119	0.029	2.850	2.399	0.831	0.098	0.033	0.354

Table 10. Correlation parameters and force-displacement parameters

References	S_1	d_1	S_2	d_2	S_3	d_3
	(kN)	(mm)	(kN)	(mm)	(kN)	(mm)
Morandi et al. [14]	355	2.882	395	6.211	270	24.173
Da Porto et al. [10]	320	1.940	361	4.315	187	26.475
Colangelo [6]	131	1.290	145	2.520	50	26.112
Bergami & Nuti [12]	140	1.166	155	2.722	48	26.960
Verderame et al. [13]	89	1.358	104	2.650	29	24.469
Sigmund & Penava [9]	79	1.553	87	3.482	33	27.975
Cavaleri & Di Trapani [11]	73	0.547	88	1.684	31	24.994

Table 11. Final axial force- axial displacement data calculated for the blind test specimen equivalent struts.

It can be firstly observed that the accuracy of each model in reproducing the experimental responses is different for the different cases. For example, while for the test by da Porto et al. [10] **(Fig. 11b),** Colangelo [6] **(Fig. 11c)** and Verderame [13] **(Figs. 11e-f)**, all the models performed with similar reliability, very significant differences in the predictions are recognized for the test by Morandi et al. [14] **(Fig. 11a)**. However, it should be also recognized that data-driven empirical models as the proposed one and the one by Di Trapani et al. [33], performed with noticeable reliability for all the considered tests. On the other hand, the models by Panagiotakos and Fardis [35]**,** Dolsek and Fajfar [38] and De Risi et al. [32] have shown good predictive capacity in 5 out of 8 tests, while they led to significant strength overestimation in the tests by Morandi et al. [14] **(Fig. 11a),** Bergami and Nuti [12] **(Fig. 11d)** and Sigmun & Penava [9]**(Fig. 11g)**. For the model by Panagiotakos and Fardis [35] and Dolsek and Fajfar [38] this is justified by the fact that the estimation of the strength capacity by these models is obtained considering a single collapse mode, leading to incorrect evaluations in all the cases in which a different mechanism develops. A confirmation of this comes observing the performance of the model by Bertoldi et al. [36] and Sassun et al. [39], which instead, based on their mechanism-sensitive formulation, resulted more effective in general with respect to the peak-strength estimation, although they still give a peak strength overestimation in 2 out of 8 cases. Another noteworthy issue is related to the softening branch, which is in general more accentuated by Panagiotakos and Fardis [35] and Dolsek and Fajfar [38] models, But while for the former this can be calibrated by a stiffness coefficient, the assumption by Dolsek and Fajfar [38] of an ultimate displacement of 5 times the peak one is generally not acceptable for more ductile infilled frames. The forced prediction of a brittle behaviour is accentuated by the low or null residual strength provided by these models, which instead it has been found to range between 0.25 and 0.8 the peak strength, as it can be deducted from the η coefficients reported in **Tables 4, 6** and **10**. In conclusion it can be observed that data-driven empirical models, including the proposed one, resulted more reliable with respect to the mechanics-based in predicting the lateral response of an infilled frame. This can be reasonably justified by two main factors. The first is that their calibration is analytically updated in consideration of a large number of parameters characterizing both the frame and the infill. More-

over, the analytical equations used to calibrate the model are based on robust correlations considering a significant number of experimental and numerical tests. The second aspect to take into account, is that the mechanics-based models here considered, despite largely employed in the practice, have been validated on a reduced number of experimental tests with respect to those available currently, and therefore they can only reflect well the behaviour of infilled frames having similar characteristics to those at the base of their validation.
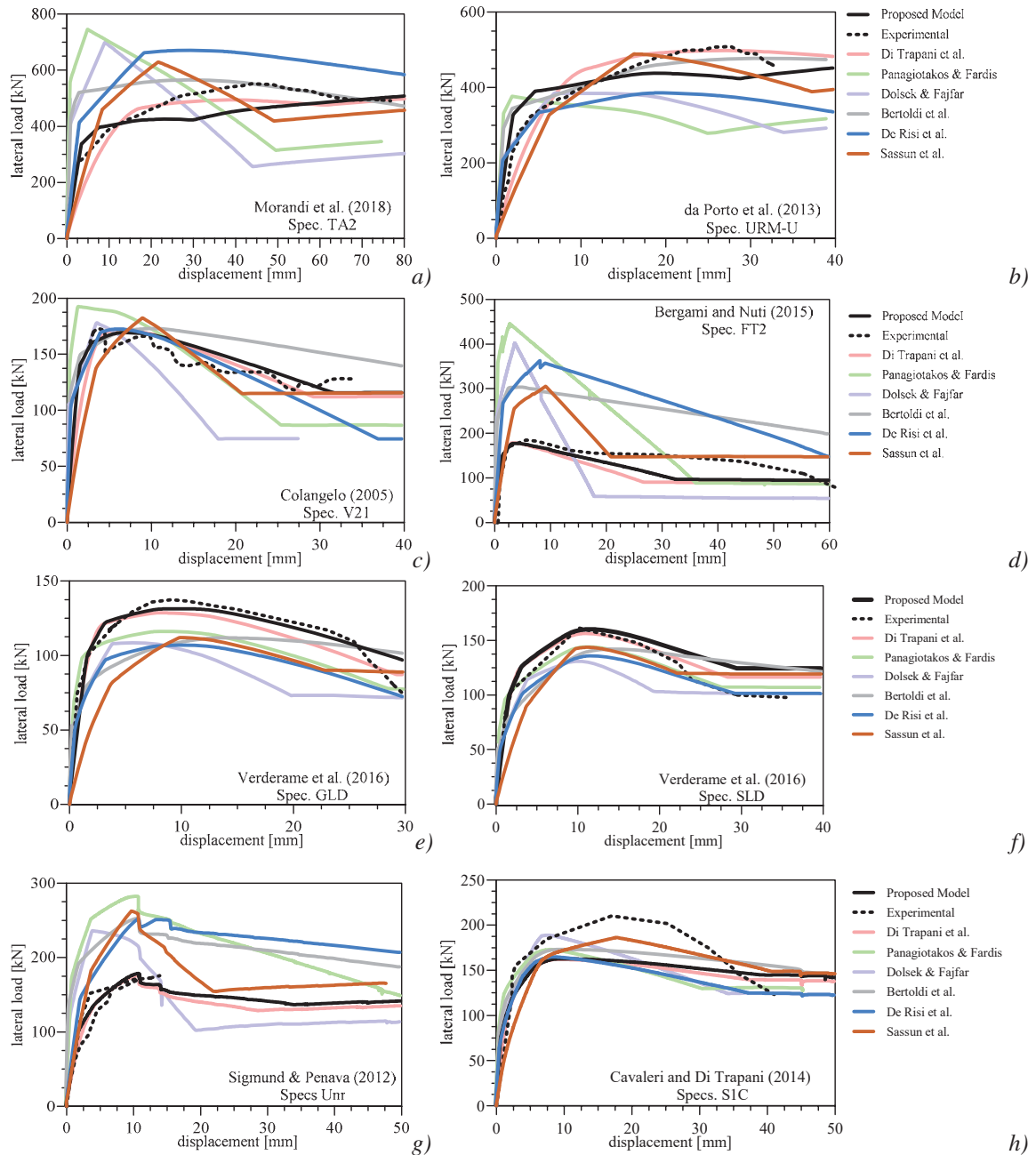
Figure 11. Blind validation tests of the proposed model with experimental test results: a) Morandi et al. (TA-2) [14]; b) da Porto et al. (URM-U)[10]; c) Colangelo (V21)[6]; d) Bergami and Nuti (FT-2)[12]; e-f) Verderame et al. (GLD-SLD)[13]; g) Sigmund & Penava [9] (Spec Unr); h) Cavaleri and Di Trapani [11] (Spec S1C)

7 CONCLUSIONS

Assessment of inelastic response of infilled frames is not straightforward. Phenomenological models have to summarize a large number of variables into a relatively simple model. The flexibility of available strut models to update their force-displacement (or stress-strain) response, as a function of the different potential failure damage mechanisms occurring for infilled frame, is fundamental to get reliable predictions. The uncertainty in predicting the collapse mode, which depends on a large amount of geometric and mechanical parameters, propagates in the reliability of estimations.

In consideration of this, the paper has shown a proposal for a new single equivalent strut model based on axial-force/axial-displacement element relationship of the strut. The model can be easily implemented in most of the finite element codes handling nonlinear analysis of frame structures. The major advantage of the proposed model is that the force-displacement relationship is modulated by four analytical correlation equations linking the geometrical and mechanical features of an infilled frame to the force-displacement parameters. The correlation equations are derived from a robust data-set realized including experimental data and refined numerical simulations.

Validation tests have been carried out against eight experimental test data different from those used to define the empirical data-set. Results have demonstrated the predictive reliability of the proposed model and of the empirical relationships used to define it. This suggests the proposed approach as an effective methodology when performing nonlinear static analyses for the assessment of seismic performance, and also highlights the potential use of correlation equations as design tools for the performance-based design of the infilled frames. The same tests are used to carry out a comparison with six additional equivalent-strut models available in the literature besides the proposed one. Results have shown a major reliability of data-driven models because of the flexibility of the case-by-case calibration provided. On the other hand, the lower reliability of mechanics-based model is justified by the reduced number of experimental tests available when they were validated.

REFERENCES

[1] Pires F., Carvalho E.C. The behaviour of infilled reinforced concrete frames under horizontal cyclic loading. *Proceedings of the 10th world conference on earthquake engineering*, Madrid; 1992.

[2] Mehrabi A.B., Shing P.B. Finite element modelling of masonry-infilled RC frames. *Journal of Structural Engineering, 123(5), 604-13*; 1996.

[3] Calvi G.M., Bolognini D. Seismic response of reinforced concrete frames infilled with weakly reinforced masonry panels. *J Earthq Eng;5(02):153–85*; 2001.

[4] Al-Chaar G., Issa M., Sweeney S. Behavior of Masonry-Infilled Nonductile Reinforced Concrete Frames. *J. Struct. Eng., 128:1055-1063*; 2002.

[5] Papia M., Cavaleri L., Fossetti M. Infilled frames: developments in the evaluation of the stiffening effect of infills. *Structural engineering and mechanics, 16(6), 675-93*; 2003.

[6] Colangelo F. Pseudo-dynamic seismic response of reinforced concrete frames infilled with non-structural brick masonry. *Earthq Eng Struct Dyn,34, 1219–1241*; 2005.

[7] Kakaletsis D.J., Karayannis C.G. Experimental investigation of infilled reinforced concrete frames with openings. *ACI Structural Journal, 102(2), 132-141*; 2009.

[8] Stylianidis K.C. Experimental investigation of masonry infilled R/C frames. *Open Constr Build Technol J;6(Suppl. 1-M13):194–212*; 2012.

[9] Sigmund V., Penava D. Experimental study of masonry infilled R/C frames with opening. *Proceedings of the 15WCEE, Lisbon, Portugal*; 2012

[10] da Porto F., Guidi M., Dalla Benetta N., Verlato F. Combined in-plane/out-of-plane experimental behaviour of reinforced and strengthened infill masonry walls. *12th Canadian Masonry Symposium, June 2-5, Vancouver, Canada*; 2013.

[11] Cavaleri L., Di Trapani F. Cyclic response of masonry infilled RC frames: Experimental results and simplified modeling. *Soil Dynamics and Earthquake Engineering, 65, 224–242*; 2014.

[12] Bergami A. V., Nuti C. Experimental tests and global modeling of masonry infilled frames. *Earthquakes and Structures, April, 1-24;* 2015.

[13] Verderame G.M., Ricci P., Del Gaudio C., De Risi M.T. Experimental tests on masonry infilled gravity- and seismic-load designed RC frames. *16th international brick and block masonry conference, IBMAC 2016; p. 1349–58*; 2016.

[14] Morandi P., Hak S., Magenes G. In-plane Experimental Response of Strong Masonry Infills. *Engineering Structures, 156, 503-521*; 2018.

[15] Celarec D., Ricci P., Dolšek M. The sensitivity of seismic response parameters to the uncertain modelling variables of masonry-infilled reinforced concrete frames. *Eng Struct , 35: 165–177*; 2012.

[16] Uva G., Raffaele D., Porco F., Fiore A. On the role of equivalent strut models in the seismic assessment of infilled RC buildings. *Engineering Structures, 42, 83–94*; 2012.

[17] Fiore A., Porco F., Raffaele D., Uva G. About the influence of the infill panels over the collapse mechanisms active under pushover analyses: Two case studies. *Soil Dynamics and Earthquake Engineering, 39, 11–22*; 2012.

[18] Asteris P.G., Repapis C.C., Tsaris A.K., Di Trapani F., Cavalieri L. Parameters affecting the fundamental period of infilled RC frame structures. *Earthquake and Structures, 9(5), 999-1028*; 2015.

[19] Asteris P.G., Cavaleri L., Di Trapani F., Sarhosis V. A macro-modelling approach for the analysis of infilled frame structures considering the effects of openings and vertical loads. *Structure and Infrastructure Engineering, 12(5), 551-566*; 2016.

[20] Martinelli E., Lima C., De Stefano G. A simplified procedure for Nonlinear Static Analysis of masonry infilled RC frames. *Engineering Structures, 101, 591–608*; 2015.

[21] Cavaleri L., Di Trapani F., Asteris P.G., Sarhosis V. Influence of column shear failure on pushover-based assessment of masonry infilled reinforced concrete framed structures: A case study. *Soil Dynamics and Earthquake Engineering, 100, 98-112*; 2017.

[22] Di Trapani F., Malavisi M. Seismic fragility assessment of infilled frames subject to mainshock/aftershock sequences using a double incremental dynamic analysis approach. *Bull Earthq Eng;17(1):211–35*; 2019.

[23] Di Trapani F., Bolis V., Basone F., Preti M.G. Seismic reliability and loss assessment of RC frame structures with traditional and innovative masonry inflls. *Eng Struct, 208:110306*; 2020a.

[24] Koutromanos I., Stavridis A., Shing P.B., Willam K. Numerical modelling of masonry-infilled RC frames subjected to seismic loads. *Computers and Structures, 89, 1026-1037*; 2011.

[25] Cavaleri L., Di Trapani F. Prediction of the additional shear action on frame members due to infills. *Bullettin of Earthquake Engineering, 13(5), 1425-1454*; 2015.

[26] Caliò I., Pantò B. A macro-element modelling approach of Infilled Frame Structures. *Computers and Structures, 143, 91-107*; 2014.

[27] Milanesi R.R., Morandi P., Magenes G. Local effects on RC frames induced by AAC masonry infills through FEM simulation of in-plane tests. *Bull of Earthq Eng, 16(1): 4053-4080*; 2018.

[28] Pantò B., Rossi P.P. A new macromodel for the assessent of the seismic response of in-filled RC frames. *Earthq Eng and Struct Dyn, 48: 792-817*; 2019.

[29] Di Trapani F., Macaluso G., Cavaleri L., Papia M. Masonry infills and RC frames interaction: literature overview and state of the art of macromodeling approach. *European Journal of Environmental and Civil Engineering, 19(9), 1059-1095*; 2015.

[30] Pasca, M., Liberatore, L., Masiani, R. Reliability of analytical models for the prediction of out-of-plane capacity of masonry infills. *Structural Engineering and Mechanics, 64(6):765-781*; 2017.

[31] Liberatore L., Noto F., Mollaioli F., Franchin P. In-plane response of masonry infill walls: Comprehensive experimentally based equivalent strut model for deterministic and probabilistic analysis. *Eng Struct, 167: 533–548*; 2018.

[32] De Risi M.T., Del Gaudio C., Ricci P., Verderame G.M. In-plane behaviour and damage assessment of masonry infills with hollow clay bricks in RC frames. *Eng Struct,168: 257–275;* 2018.

[33] Di Trapani F., Bertagnoli G., Ferrotto M.F., Gino D. Empirical equations for the direct defnition of stress-strain laws for fiber-section based macro-modeling of infilled frames. *J Eng Mech, 144(11):04018101*; 2018b.

[34] McKenna F., Fenves G.L., Scott M.H. *Open system for earthquake engineering simulation. University of California, Berkeley, CA*; 2000.

[35] Panagiotakos, T.B., Fardis, M.N. Seismic response of infilled RC frames structures. *XXI WCEE, Acapulco, Mexico*; 1996.

[36] Bertoldi S. H., Decanini L.D., Gavarini C. Telai tamponati soggetti ad azioni sismiche, un modello semplificato: confronto sperimentale e numerico. *Atti del 6 Convegno Nazionale ANIDIS, 2, Perugia*; 1993.

[37] Cavaleri, L., Fossetti, M., & Papia, M. Infilled frames: Developments in the evaluation of cyclic behaviour under lateral loads. *Structural Engineering and Mechanics*, 21, 469–494; 2005.

[38] Dolšek, M., Fajfar, P. The effect of masonry infills on the seismic response of four storey reinforced concrete frame - a deterministic assessment. *Engineering Structures, 30(7)*,1991-2001;2008.

[39] Sassun, K., Sullivan, T.J., Morandi, P., Cardone, D. Characterising the In-Plane Seismic Performance of Infill Masonry. *Bull. N. Z. Soc. Earthq. Eng. , 49, 98–115*; 2015.

[40] Di Trapani, F., Bolis, V. Basone, F., Preti M. Seismic reliability and loss assessment of RC frame structures with traditional and innovative masonry infills. *Engineering Structures*, 208, 110306; 2020.

[41] Cavaleri L., F. Di Trapani F., Ferrotto M.F. A new hybrid procedure for the definition of seismic vulnerability in Mediterranean cross-border urban areas. *Natural Hazards*, 86, no. S2, 517–541; 2017.

[42] Cavaleri, L., Di Trapani, F., Ferrotto, M.F., Davì, L. Stress-strain models for normal and high strength confined concrete: Test and comparison of literature models reliability in reproducing experimental results. *Ingegneria Sismica, 3*4(3-4), 114-137; 2017.